

Throughput of Hybrid UAV Networks with Scale-Free Topology

Zhiqing Wei, Ziyu Wang, Zeyang Meng, Ning Zhang, Huici Wu, Zhiyong Feng

Abstract—Unmanned Aerial Vehicles (UAVs) hold great potential to support a wide range of applications due to the high maneuverability and flexibility. Compared with single UAV, UAV swarm carries out tasks efficiently in harsh environment, where the network resilience is of vital importance to UAV swarm. The network topology has a fundamental impact on the resilience of UAV network. It is discovered that scale-free network topology, as a topology that exists widely in nature, has the ability to enhance the network resilience. Besides, increasing network throughput can enhance the efficiency of information interaction, improving the network resilience. Facing these facts, this paper studies the throughput of UAV Network with scale-free topology. Introducing the hybrid network structure combining both ad hoc transmission mode and cellular transmission mode into UAV Network, the throughput of UAV Network is improved compared with that of pure ad hoc UAV network. Furthermore, this work also investigates the optimal setting of the hop threshold for the selection of ad hoc or cellular transmission mode. It is discovered that the optimal hop threshold is related with the number of UAVs and the parameters of scale-free topology. This paper may motivate the application of hybrid network structure into UAV Network.

Index Terms—Unmanned Aerial Vehicle; Scale-free Network; Throughput; Scaling Law; Network Resilience

I. INTRODUCTION

In recent years, with the development of the technologies such as mobile communications, artificial intelligence, and automatic control, Unmanned Aerial Vehicles (UAVs) have been widely applied in many areas, such as reconnaissance, disaster rescue, wireless communication and logistics, due to the advantages of high maneuverability and flexibility [1]. The application of UAVs is showing a blowout trend, and the application areas are continuously expanding. However, due to the extremely limited endurance time, power, size, and the harsh environment where UAVs carry out tasks, it is difficult for a single UAV to complete tasks quickly and efficiently. Thus, the collaboration among UAV swarm is required [2]. Taking into account the harsh environment in which UAV swarm is applied, the ability of UAV swarm to defend against device faults or other possible attacks and maintain the reliability of services, namely, the network resilience [3], is of vital importance to UAV swarm. Hence, the network resilience of

UAV swarm is a key factor restricting the wide application of UAV swarm [4] [5].

On the one hand, the network topology has a fundamental impact on the resilience of UAV network. Scale-free network topology, as a topology that exists widely in nature, such as Internet and biological swarms, has attracted widespread attention. The power-law distribution of the degree of the nodes is one of the important characteristics of this kind of complex network [6], [7]. As a typical complex network, the large-scale UAV network is widely studied [8], [9], where the large-scale UAV network is a scale-free network. For example, [10] verified that the large-scale network has scale-free characteristic naturally under rules of Reynolds Boids. On the other hand, the study on scale-free structure of UAV network is of great significance to improve the network performance. Because the scale-free structure has great robustness when facing intentional attacks [11], [12]. In an asymptotic sense, all network nodes need to be destroyed in order to destroy the scale-free network, which greatly improves the stability and reliability of UAV network. Tran *et al.* [13] and Fan *et al.* [8] studied the scale-free UAV network and found that randomly removing nodes has little effect on the connectivity of UAV network, so that the network has a higher tolerance for random attacks. To this end, in order to enhance the resilience of UAV swarm, the UAV network topology with scale-free network topology has been studied in depth. In [10], inspired by the scale-free characteristics of bird flocks enhancing environmental response capabilities, Singh *et al.* studied the scale-free characteristics of UAV swarm to improve the survivability of UAV swarm.

On the other hand, the network throughput has a correlation with network resilience. The increase of network throughput will decrease the congestion probability and the communication delay. As a result, the UAV swarm has a short response time to the interruption of the network, and the network resilience is improved. In order to alleviate congestion and reduce network response time, Defense Advanced Research Projects Agency (DARPA) [14] released a project called Content-Based Mobile Edge Networking (CBMEN) to effectively improve network throughput and reduce delay. Liu *et al.* [15] modeled the relation between network resilience and network throughput, and maximized the throughput to improve the fault recovery ability of the network.

Therefore, it is shown that both network topology and network throughput can comprehensively affect the resilience of UAV network. In terms of the throughput of UAV network, Yuan *et al.* studied the impact of the mobility of UAVs on the link throughput of UAV Network [16]. Li *et al.* [17] studied the

Zhiqing Wei, Zeyang Meng, Huici Wu, and Zhiyong Feng are with Beijing University of Posts and Telecommunications, Beijing, China 100876 (email: {weizhiqing, mengzeyang, dailywu, fengzy}@bupt.edu.cn).

Ziyu Wang is with Amazon (China) Holding Company Limited, Beijing, China 100025 (email: ziyuwan@amazon.com).

Ning Zhang is with the Department of Electrical and Computer Engineering, University of Windsor, Windsor, ON, N9B 3P4, Canada. (e-mail: ning.zhang@uwindsor.ca).

Correspondence authors: Ziyu Wang, Huici Wu, and Zhiqing Wei.

throughput of air-to-air links and the multiple access channel (MAC) throughput of UAV network. Chetlur *et al.* [18] studied the outage probability of the link of three-dimensional (3D) UAV network, and analyzed the resilience of the UAV network from the perspective of reliability. Gao *et al.* [19] enhanced the throughput of UAV Network by optimizing the deployment of UAVs in 3D space. We studied the throughput of 3D UAV network in [20], discovering that the UAV network throughput is a function of the path loss factor in 3D space, the number of nodes, the factor of contact concentration, and so on. However, the throughput of UAV network with scale-free topology was seldom studied. The research on the wireless network with scale-free topology is firstly reported in [21], where the degree of node follows a power-law distribution, which is the feature of scale-free network. [21] has found the relation between network throughput and node degree. By assigning independent spectrum resources to nodes with high degrees, the throughput of the UAV network is improved. [22] and [23] are preliminary works of [21], where the distribution of node's degrees follows uniform distribution. We studied the throughput of 3D scale-free network in [24]. Compared with [21], [24] studied the impact of 3D network topology on the throughput of scale-free network. Besides, the optimal threshold of the degree is studied, and the separated resources are allocated to nodes with the degree larger than the threshold to enhance the network throughput.

To wrap up, the scale-free topology improves the resilience of UAV network, and the enhancement of the throughput of UAV network is essential to improve the resilience of UAV network. In order to improve the throughput of UAV network, a hybrid UAV network is formed with the cooperation between UAV network and ground cellular network in this paper. Hybrid network is a combination of ad hoc network and cellular network [25]. As shown in Fig. 1, when the source node and the sink node are far away, the data can be transmitted with cellular mode. On the contrary, when the source node and the sink node are close, the data can be transmitted via ad hoc mode. Kumar *et al.* proposed this model earlier in [26] and proved the improvement of network throughput through the hybrid network model.

In this paper, the throughput of the hybrid UAV network with scale-free topology is studied. The contributions of this paper are as follows.

- The 3D model is applied in this paper, which is more realistic than the two-dimensional (2D) model. The 3D model has mainly two differences compared with 2D model. Firstly, the relative relationship between UAV and base station (BS) is more practical. Considering the flight capability and spatial distribution characteristics of the UAV, the BS is located on the 2D plane, namely the ground, and the UAV is located in a the cubic 3D space, rather than simply assuming that the UAV and the BS are deployed on the same plane. Secondly, the difference on dimension causes the difference on power and segmentation of theoretical results between two models.
- The three dimensions of the scale-free characteristics are considered in the hybrid network, i.e., the probability of

source nodes selecting contact group members follows the power-law distribution corresponding to the distance, the probability of source nodes communicating with contact group members follows the power-law distribution corresponding to the distance, and the number of contact group members follows a power-law distribution. Compared with the existing researches on the throughput of hybrid scale-free networks, such as [23], the scale-free characteristic of the number of members in the contact group, i.e., the power-law exponent γ , is taken into consideration in this paper.

This paper is organized as follows. In Section II, the network model of hybrid UAV network with scale-free topology is introduced. In Section III, the throughput of hybrid UAV Network with scale-free topology is derived. The numerical results of the analytical results are shown in Section IV. Finally, in Section V, we summarize this paper.

II. NETWORK MODEL

The hybrid network is the combination of ad hoc network and cellular network. The cellular network serves as backbone network. As illustrated in Fig. 1, in hybrid UAV network, the BSs are distributed on ground, and the UAVs are uniformly distributed in the unit cube¹. When the distance between source and destination is small, the information flow goes through ad hoc mode. However, when the distance between source and destination is large, the information flow goes through cellular mode.

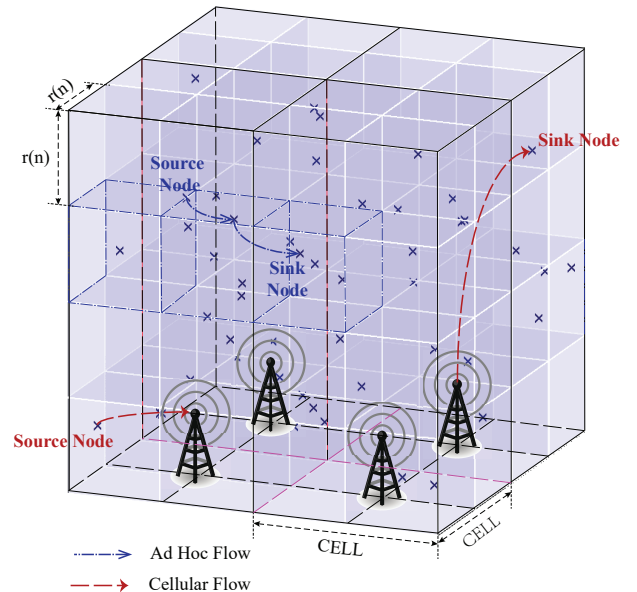


Fig. 1. Multi-hop routing strategy from source to destination.

¹The square-area assumption and the division method of a 2D plane is described in [28], which is equal to a Voronoi tessellation satisfying Remark 5.6 in [28]. The division method guarantees that there is at least one node in each small square when the number of nodes n tends to infinity. Similarly, the division method of 3D unit cube in this paper can be analogized from the result mentioned above, which is also applied in [29].

A. Communication model

1) *Interference model*: In the UAV network, n UAVs are uniformly distributed in the unit cube. The unit cube is divided into small cubes with side length $\Theta \left(\left(\frac{\log n}{n} \right)^{\frac{1}{3}} \right)^2$. According to Fig. 1, each small cube contains at least one node with high probability (*w.h.p.*) if the transmission range $r(n)$ between the two nodes is as follows [27].

$$r(n) = \Theta \left(\left(\frac{\log n}{n} \right)^{\frac{1}{3}} \right). \quad (1)$$

We apply the *protocol model* [30] for interference management. Assuming that the 3D Cartesian coordinates of the nodes i, j, k are X_i, X_j, X_k respectively, two nodes can communicate successfully when

$$|X_i - X_j| < r(n), \quad (2)$$

and the other nodes that transmit on the same frequency band satisfy the condition

$$|X_k - X_j| > (1 + \Delta) r(n), \quad (3)$$

where $\Delta > 0$ is the guard zone factor.

2) *Multiple access control*: In order to avoid multiple access interference, time division multiple access (TDMA) is adopted. Suppose that the side length of each small cube is $c_1 r(n)$, where c_1 is a constant smaller than 1 to ensure that all nodes in the neighboring cubes are within the transmission range. According to the interference model in Section II-A1, only the nodes within the intervals of M cubes are allowed to communicate simultaneously, where $M \geq \frac{2+\Delta}{c_1}$. Then M^3 cubes become a cluster, and the cubes in the entire cluster are traversed in M^3 time slots in a round-robin scheduling method. The TDMA scheme in this paper is denoted by M^3 -TDMA scheme. As shown in Fig. 2, the green cubes are located in different clusters, and the nodes in these cubes can transmit data at the same time.

Note that the analytical results under such protocol are also applicable to other multiple access control (MAC) protocol. Some studies have proved that MAC protocol will not affect the throughput scaling law. For example, [31] studied the throughput bound scaling law of ad hoc network under Carrier Sense Multiple Access with Collision Avoid (CSMA/CA) protocol, which proved that the ad hoc network with CSMA/CA protocol has the same throughput scaling law as the ad hoc network with TDMA protocol.

3) *Data flows*: As illustrated in Fig. 1, BSs are distributed in a unit square on ground. The unit square is divided into $m = \Theta \left(\left(\frac{\log n}{n} \right)^{-\frac{2}{3}} \right)$ cells. And there is a BS at the center of each cell. The volume of each cell is $1/m$. A UAV is associated with the nearest BS. The BSs are connected via optical fiber with high throughput. Hence, there are no throughput limitations among the BSs. In Fig. 1, there are

²In this paper, $f(n) = O(g(n))$ means that $\lim_{n \rightarrow \infty} \frac{f(n)}{g(n)} < \infty$; $f(n) = \Omega(g(n))$ means that $g(n) = O(f(n))$; $f(n) = \Theta(g(n))$ means that $f(n) = O(g(n))$ and $g(n) = O(f(n))$, which is also denoted by $f(n) \equiv g(n)$.

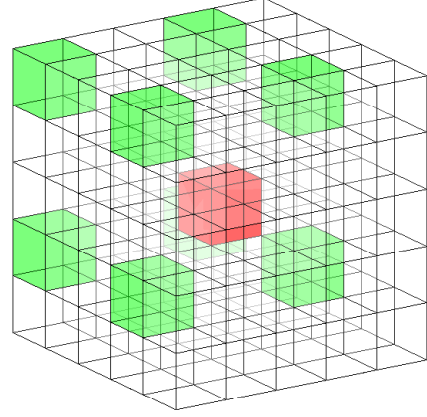


Fig. 2. The illustration of TDMA model where nodes in green cubes can transmit data at the same time. In this figure, we assume that the source node is located in the red cube.

two kinds of information flows, namely, ad hoc flow adopting multi-hop transmission and cellular flow adopting BSs to transmit data. The total bandwidth W bits per second (bps) is divided into two parts, with W_a bps allocated to ad hoc flows and W_c bps allocated to cellular flows. Thus, we have

$$W = W_a + W_c. \quad (4)$$

4) *Routing scheme*: The L -routing scheme [32] is applied in this paper. If the number of hops from source to destination is smaller than L , the ad hoc transmission mode is adopted. Otherwise, the information is transmitted via cellular mode. For the ad hoc information flow denoted by blue line in Fig. 1, the straight line routing is adopted, the information is transmitted from source to destination through the cubes passed through by the line connecting source and destination. For cellular flow, the source transmits data to the nearby BS. Then, the data is transmitted to the BS associated to destination and finally forwarded to the destination.

B. Scale-free network model

The network model of scale-free network consists of the distance based contact group model, the communication model of nodes and the distribution of the number of members in contact group. The contact group of node S is a collection of destination nodes that communicate with node S over a period of time. The distance based contact group construction describes the probability model of source node with specific contact group. The communication model describes the communication probability of nodes in contact groups. The number of members in contact group describes the probability model of the number of contact group members.

1) *Distance based contact group construction*: Source node S selects any other nodes as the member of its contact group G with a power-law distribution probability [33]. With d_i denoting the distance between S and node o_i , the probability that o_i is selected as a member of contact group follows power-

law distribution as follows.

$$P(D = o_i) = d_i^{-\alpha}, \quad (5)$$

where α is a factor representing the concentration of the network, which is named as *concentration factor* in this paper. When α is large, the selection probability of contact group members attenuates greatly with distance, and members in the contact group tend to be located near the source node. The selection of the member of contact group is an independent process. Thus, the probability that G consists of nodes $o_{g_1}, o_{g_2}, \dots, o_{g_q}$ is [21]

$$\Pr(G = \{o_{g_1}, \dots, o_{g_q}\}) = \frac{d_{g_1}^{-\alpha} \dots d_{g_q}^{-\alpha}}{\sum_{1 \leq i_1 < \dots < i_q \leq n} d_{i_1}^{-\alpha} \dots d_{i_q}^{-\alpha}}. \quad (6)$$

The denominator is an elementary symmetric polynomial and can be denoted as [21]

$$\sigma_q(\mathbf{d}_n) = \sum_{1 \leq i_1 < \dots < i_q \leq n} d_{i_1}^{-\alpha} \dots d_{i_q}^{-\alpha}, \quad (7)$$

where $\mathbf{d}_n = (d_1^{-\alpha}, \dots, d_n^{-\alpha})$ is an n -dimensional vector. Calculating the synthesis of all combinations, the probability of an arbitrary particular node o_k being a member of G is denoted by [21]

$$\Pr(o_k \in G) = \frac{d_k^{-\alpha} \sigma_{q-1}(\mathbf{d}_n^{\bar{k}})}{\sigma_q(\mathbf{d}_n)}, \quad (8)$$

where $\mathbf{d}_n^{\bar{k}}$ is the $(n-1)$ -dimensional vector except of the k -th element $d_k^{-\alpha}$.

2) *Communication model of nodes*: With the contact group established, the probability of source node S choosing the destination node inside the contact group G to communicate also follows power-law distribution. The probability of node o_i selected to be the destination is $d_i^{-\beta}$, where the factor β reveals the communication activity level of the contact group, which is named as *communication activity factor* in this paper. Thus, the probability that o_k is the destination node D in G is

$$\Pr(D = o_k | o_k \in G) = \frac{d_k^{-\beta}}{\sum_{i=1}^q d_{g_i}^{-\beta}} = \frac{d_k^{-\beta}}{\sigma_1(\mathbf{d}_q)}, \quad (9)$$

where $\mathbf{d}_q = (d_{g_1}^{-\beta}, \dots, d_{g_q}^{-\beta})$. When β is large, the probability of communication destination selection decreases greatly with distance, and the source node tends to communicate with the node at a close location.

3) *Number of members in contact group*: The number of members in the contact group, which is the degree of a node, is denoted by d . Then, the probability density function (PDF) of d follows a power-law distribution as follows.

$$P(d = q) \propto q^{-\gamma}, \quad (10)$$

where q is a positive integer, γ is the power-law exponent, which is named as *clustering factor* in this paper. $A \propto B$ means that A is proportional to B. When γ is large, the number of contact group members is small.

Assume that each source node S has a contact group G and the number of G 's members is a random variable Q . The

probability that G has q ($q = 1, 2, \dots, n$) members is [21]

$$\Pr(Q = q) = \frac{q^{-\gamma}}{\sum_{q=1}^{n-1} q^{-\gamma}} = \frac{q^{-\gamma}}{\sigma_1(\mathbf{q})}, \quad (11)$$

where $\sigma_1(\mathbf{q})$ is an elementary symmetric polynomial, with $\mathbf{q} = \{1^{-\gamma}, 2^{-\gamma}, \dots, (n-1)^{-\gamma}\}$.

III. THROUGHPUT OF HYBRID UAV NETWORK

The per-node throughput of ad hoc mode is denoted by λ_a^n bps. The per-node throughput of cellular mode is denoted by λ_c^n bps. Assuming that the number of ad hoc flows and cellular flows is N_a and N_c respectively, the network throughput is ³

$$\lambda = \lambda_a + \lambda_c = N_a \lambda_a^n + N_c \lambda_c^n. \quad (12)$$

A. Network throughput of cellular mode

The network throughput of cellular mode is related with the number of BSs m and the bandwidth W_c . We have the following theorem.

Theorem 1. *The network throughput of cellular mode λ_c satisfies the following equality.*

$$\lambda_c = \Theta(mW_c). \quad (13)$$

Proof: According to the bandwidth allocation strategy in (4), the network throughput of each cell has upper bound $\lambda_c^m = O(W_c)$. Assuming that there are x_{cells} cells sharing the same bandwidth W_c , the lower bound of the throughput of each cell is $\lambda_c^m = \Omega(W_c/x_{cells})$, where x_{cells} is a constant that is independent with n and m [34]. Hence, the network throughput of each cell is $\lambda_c^m = \Theta(W_c)$. Because there are totally m cells, the network throughput contributed by cellular mode is $\lambda_c = m\lambda_c^m = \Theta(mW_c)$. ■

B. Network throughput of ad hoc mode

The network throughput of ad hoc mode depends on the average number of hops of ad hoc flows passing through each small cube $E[F]$, where F is the number of ad hoc flows contained in each small cube.

Theorem 2. *The per-node throughput of ad hoc mode satisfies the following equation.*

$$\lambda_a^n \equiv \Theta\left(\frac{W_a}{E[F]M^3}\right) = \Theta\left(\frac{W_a}{E[F]}\right). \quad (14)$$

Proof: As mentioned above, the side length of the small cube is $c_2 r(n) = \Theta\left((\log n/n)^{\frac{1}{3}}\right)$. Supposing that the number of hops from source to destination is X , where X is a random variable, the average number of hops of one ad hoc flow is $E[X]$. Therefore, the average number of hops of all the ad hoc flows is $N_a E[X]$. Because of the random distribution of nodes, each cube contains $E[F] = N_a E[X]V$ transmission flows, where $V = (c_2 r(n))^3$ is the volume of the small cube. According to the *Multiple Access Protocol* in Section II, the

³The per-node throughput is denoted by superscript 'n', while the throughput of the network has no superscript. The subscript 'a' denotes ad hoc mode and the subscript 'c' denotes cellular mode.

average bandwidth of each slot is $\frac{W_a}{M^3}$. Therefore, the per-node throughput λ_a^n of each node is

$$\lambda_a^n \equiv \Theta \left(\frac{W_a}{E[F] M^3} \right) = \Theta \left(\frac{W_a}{E[F]} \right). \quad (15)$$

Therefore, the network throughput contributed by ad hoc mode is $\lambda_a = N_a \lambda_a^n$. ■

C. Node and flow classification

The structure of cubes with x hops away from a source node is a octahedron, as the shaded cubes illustrated in Fig. 3, which consists of $4x^2 + 2$ cubes. $\Pr(X = x)$ represents the

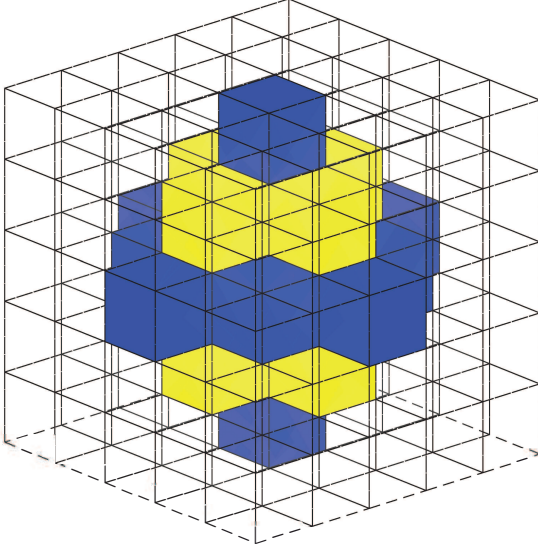


Fig. 3. Cubes with x hops away from the source node, where $x = 2$

probability that the distance from the destination node D to the source node S is x hops. According to (6) in [24], we have

$$\Pr(X = x) = \sum_{l=1}^{4x^2+2} \sum_{o_k \in c_l} \Pr(D = o_k), \quad (16)$$

where c_l is the set of the nodes in the cube that is x hops away from the source node and o_k is the destination node within it. Because the nodes are randomly distributed, the probability that any node is located in the cube is $r^3(n)$. Therefore, the number of nodes contained in c_l is $nr^3(n)$ on average. Thus we have

$$\Pr(X = x) = \sum_{l=1}^{4x^2+2} nr^3(n) \Pr(D = o_k). \quad (17)$$

Because of the same power-law distribution as [24], we use the same symbol as [24], where α represents the concentration of the network, β reveals the communication activity level, and γ is the clustering factor. According to (9) (17) in this paper and (7) in [24], we have the following probability

$$\Pr(X = x) = \sum_{l=1}^{4x^2+2} \sum_{o_k \in c_l} \sum_{q=1}^{n-1} \frac{q^{-\gamma} d_k^{-\alpha-\beta} \sigma_{q-1}(\mathbf{d}_n^k)}{\sigma_1(\mathbf{q}) \sigma_1(\mathbf{d}_q) \sigma_q(\mathbf{d}_n)}. \quad (18)$$

When the destination node is in the regions that are within L hops to the source node S , the data flow is forwarded with ad hoc mode. The probability that a flow is an ad hoc flow is denoted by \Pr^a , then we have

$$\begin{aligned} \Pr^a &= \sum_{x=1}^L \Pr(X = x) \\ &= \sum_{x=1}^L \sum_{l=1}^{4x^2+2} \sum_{o_k \in c_l} \sum_{q=1}^{n-1} \frac{q^{-\gamma} d_k^{-\alpha-\beta} \sigma_{q-1}(\mathbf{d}_n^k)}{\sigma_1(\mathbf{q}) \sigma_1(\mathbf{d}_q) \sigma_q(\mathbf{d}_n)}. \end{aligned} \quad (19)$$

When the destination node is in the regions that are more than L hops to the source node, the data flow is forwarded with cellular mode. According to [24], the maximum number of hops of each flow is $\Theta(r^{-1}(n))$. The probability that a flow is a cellular flow is denoted by \Pr^c . Then we have

$$\Pr^c = \sum_{x=L+1}^{r^{-1}(n)} \sum_{l=1}^{4x^2+2} \sum_{o_k \in c_l} \sum_{q=1}^{n-1} \frac{q^{-\gamma} d_k^{-\alpha-\beta} \sigma_{q-1}(\mathbf{d}_n^k)}{\sigma_1(\mathbf{q}) \sigma_1(\mathbf{d}_q) \sigma_q(\mathbf{d}_n)}. \quad (20)$$

The feature of scale-free topology shows that a few nodes have a large number of associated nodes. Thus, a threshold q_0 of node degree is chosen that classifies all the nodes into two classes. The nodes whose degree $q > q_0$ are leader nodes, and the nodes whose degree $q \leq q_0$ are normal nodes. We define \Pr_1^a as the probability for leader nodes transmitting with ad hoc mode and \Pr_1^c for leader nodes transmitting with cellular mode, then

$$\Pr_1^a = \sum_{x=1}^L \sum_{l=1}^{4x^2+2} \sum_{o_k \in c_l} \sum_{q=q_0+1}^{n-1} \frac{q^{-\gamma} d_k^{-\alpha-\beta} \sigma_{q-1}(\mathbf{d}_n^k)}{\sigma_1(\mathbf{q}) \sigma_1(\mathbf{d}_q) \sigma_q(\mathbf{d}_n)}, \quad (21)$$

$$\Pr_1^c = \sum_{x=L+1}^{r^{-1}(n)} \sum_{l=1}^{4x^2+2} \sum_{o_k \in c_l} \sum_{q=q_0+1}^{n-1} \frac{q^{-\gamma} d_k^{-\alpha-\beta} \sigma_{q-1}(\mathbf{d}_n^k)}{\sigma_1(\mathbf{q}) \sigma_1(\mathbf{d}_q) \sigma_q(\mathbf{d}_n)}. \quad (22)$$

Similarly, we define \Pr_2^a as the probability for normal nodes transmitting with ad hoc mode and \Pr_2^c as the probability for normal nodes transmitting with cellular mode, then

$$\Pr_2^a = \sum_{x=1}^L \sum_{l=1}^{4x^2+2} \sum_{o_k \in c_l} \sum_{q=1}^{q_0} \frac{q^{-\gamma} d_k^{-\alpha-\beta} \sigma_{q-1}(\mathbf{d}_n^k)}{\sigma_1(\mathbf{q}) \sigma_1(\mathbf{d}_q) \sigma_q(\mathbf{d}_n)}, \quad (23)$$

$$\Pr_2^c = \sum_{x=L+1}^{r^{-1}(n)} \sum_{l=1}^{4x^2+2} \sum_{o_k \in c_l} \sum_{q=1}^{q_0} \frac{q^{-\gamma} d_k^{-\alpha-\beta} \sigma_{q-1}(\mathbf{d}_n^k)}{\sigma_1(\mathbf{q}) \sigma_1(\mathbf{d}_q) \sigma_q(\mathbf{d}_n)}. \quad (24)$$

D. Analysis of average number of hops

As for \Pr_1^a and \Pr_1^c , we have the following theorem.

Theorem 3. \Pr_1^a and \Pr_1^c satisfy the following equations.

$$\Pr_1^a \equiv \begin{cases} \Theta(r^3(n) L^{3-\beta}) & 0 \leq \beta < 3 \\ \Theta(r^3(n) \ln L) & \beta = 3 \\ \Theta(r^3(n)) & \beta > 3 \end{cases} \quad (25)$$

$$\Pr_1^c \equiv \begin{cases} \Theta(r^\beta(n) - r^3(n) L^{3-\beta}) & 0 \leq \beta < 3 \\ \Theta\left(r^3(n) \ln\left(\frac{1}{Lr(n)}\right)\right) & \beta = 3 \\ \Theta(r^3(n)) & \beta > 3 \end{cases} \quad (26)$$

Proof: Please refer to Appendix A. ■

Theorem 4. The orders of \Pr_2^a and \Pr_2^c are listed in Table I and Table II, respectively.

TABLE I
THE PROBABILITY OF NORMAL AD HOC FLOW Pr_2^a

| $\alpha + \beta \backslash \alpha$ | $0 \leq \alpha < 3$ | $\alpha = 3$ | $\alpha > 3$ |
|------------------------------------|---|--|------------------------|
| $\gamma > 1$ | | | |
| $0 \leq \alpha + \beta < 3$ | $\Theta(r^{3-\alpha}(n)L^{3-\alpha-\beta})$ | - | - |
| $\alpha + \beta = 3$ | $\Theta(r^{3-\alpha}(n) \ln L)$ | $\Theta(\log_{r^{-1}(n)} L)$ | - |
| $\alpha + \beta > 3$ | $\Theta(r^{3-\alpha}(n))$ | $\Theta(\ln^{-1}(r^{-1}(n)))$ | $\Theta(1)$ |
| $0 \leq \gamma \leq 1$ | | | |
| $0 \leq \alpha + \beta < 3$ | $\Theta(n^{\gamma-1}r^{3-\alpha}(n)L^{3-\alpha-\beta})$ | - | - |
| $\alpha + \beta = 3$ | $\Theta(n^{\gamma-1}r^{3-\alpha}(n) \ln L)$ | $\Theta(n^{\gamma-1} \log_{r^{-1}(n)} L)$ | - |
| $\alpha + \beta > 3$ | $\Theta(n^{\gamma-1}r^{3-\alpha}(n))$ | $\Theta(n^{\gamma-1} \ln^{-1}(r^{-1}(n)))$ | $\Theta(n^{\gamma-1})$ |

TABLE II
THE PROBABILITY OF NORMAL CELLULAR FLOW Pr_2^c

| $\alpha + \beta \backslash \alpha$ | $0 \leq \alpha < 3$ | $\alpha = 3$ | $\alpha > 3$ |
|------------------------------------|--|---|--|
| $\gamma > 1$ | | | |
| $0 \leq \alpha + \beta < 3$ | $\Theta(r^\beta(n) - r^{3-\alpha}(n)L^{3-\alpha-\beta})$ | - | - |
| $\alpha + \beta = 3$ | $\Theta(r^{3-\alpha}(n) \ln(r^{-1}(n)L^{-1}))$ | $\Theta(1 - \log_{r^{-1}(n)} L)$ | - |
| $\alpha + \beta > 3$ | $\Theta(r^\beta(n) - r^{3-\alpha}(n)L^{3-\alpha-\beta})$ | $\Theta(\ln^{-1}(r^{-1}(n)) (r^\beta(n) - L^\beta))$ | $\Theta(r^{\alpha+\beta-3}(n) - L^{3-\alpha-\beta})$ |
| $0 \leq \gamma \leq 1$ | | | |
| $0 \leq \alpha + \beta < 3$ | $\Theta(n^{\gamma-1}(r^\beta(n) - r^{3-\alpha}(n)L^{3-\alpha-\beta}))$ | - | - |
| $\alpha + \beta = 3$ | $\Theta(n^{\gamma-1}r^{3-\alpha}(n) \ln(r^{-1}(n)L^{-1}))$ | $\Theta(n^{\gamma-1}(1 - \log_{r^{-1}(n)} L))$ | - |
| $\alpha + \beta > 3$ | $\Theta(n^{\gamma-1}(r^\beta(n) - r^{3-\alpha}(n)L^{3-\alpha-\beta}))$ | $\Theta(n^{\gamma-1} \ln^{-1}(r^{-1}(n)) (r^\beta(n) - L^\beta))$ | $\Theta(n^{\gamma-1}(r^{\alpha+\beta-3}(n) - L^{3-\alpha-\beta}))$ |

Proof: Please refer to Appendix B. ■

Using the results of Pr_1^a in (25), Pr_1^c in (26), Pr_2^a in Table I, and Pr_2^c in Table II, the number of ad hoc flows N_a and the number of cellular flows N_c can be derived. When $\gamma > 1$, the results of N_a and N_c are shown in (27) and (28).

Therefore, whether the flows are dominated by ad hoc flows or cellular flows is influenced by L in the routing strategy. It is observed that when $\alpha > 3$, N_a increases linearly with n . Because when α increases, contact group members of source node gather around the source node, so that the number of hops needed for communication tends to be smaller than L , thus the number of ad hoc flows increases with n . Besides, on account of $L = O(r^{-1}(n))$ and $L = \Omega(1)$, we have $N_a + N_c \equiv \Theta(n)$.

Theorem 5. *The average number of hops of ad hoc flows passing through each cube, namely $E[F]$, is $(n\text{Pr}^a) \times (\frac{1}{\text{Pr}^a} E'[X]) \times r^3(n)$, where Pr^a is the probability for nodes transmitting with ad hoc mode.*

Proof: As mentioned in Section III-B, $E[F] = N_a E[X] V$, where $V \equiv r^3(n)$.

The total number of hops of all ad hoc flows is denoted by X_{total} . The number of hops of flow i is denoted by X_i . Then, we have

$$E[X_{total}] = E\left[\sum_{i=1}^{N_a} X_i\right] = \sum_{i=1}^{N_a} E[X_i]. \quad (29)$$

Suppose that $X_i (i \in \{1, 2, \dots, N_a\})$ are independent and identically distributed (i.i.d.), and X has the same distribution with X_i . Then, we have $E[X_{total}] = N_a E[X]$. On the

condition of unbiased estimation, $E[X_{total}] = N_a E[X]$. Therefore, for each cube, $E[F] = N_a E[X] V$, where $E[X]$ is as (30).

$$\begin{aligned} E[X] &= \sum_{x=1}^L x \Pr(X = x | \text{The flow is ad hoc flow}) \\ &= \sum_{x=1}^L x \frac{\Pr(X = x)}{\text{Pr}^a} \\ &= \frac{1}{\text{Pr}^a} \sum_{x=1}^L x \Pr(X = x). \end{aligned} \quad (30)$$

Suppose that $E'[X] = \sum_{x=1}^L x \Pr(X = x)$, we have $E[X] = E'[X] / \text{Pr}^a$. We divide $E'[X]$ into two parts according to the threshold q_0 , i.e. $E'[X] = E'_1[X] + E'_2[X]$, where $E'_1[X]$ represents the average number of hops of the flows starting from leader nodes, and $E'_2[X]$ represents the average number of hops of the flows starting from normal nodes.

Substituting (18) and (19) into $E'_1[X]$ and $E'_2[X]$, $E'_1[X]$ is as follows.

$$E'_1[X] = \begin{cases} \Theta(r^3(n)L^{4-\beta}) & 0 \leq \beta < 4 \\ \Theta(r^3(n) \ln L) & \beta = 4 \\ \Theta(r^3(n)) & \beta > 4 \end{cases} \quad (31)$$

When $\gamma > 1$, $E'_2[X]$ is

$$N_\alpha = \begin{cases} \Theta(nr^3(n)L^{3-\beta} + nr^{3-\alpha}(n)L^{3-\alpha-\beta}) & 0 \leq \alpha < 3, 0 \leq \alpha + \beta < 3 \\ \Theta(nr^3(n)L^{3-\beta} + nr^{3-\alpha}(n)\ln L) & 0 \leq \alpha < 3, \alpha + \beta = 3 \\ \Theta(nr^3(n)L^{3-\beta} + nr^{3-\alpha}(n)) & 0 \leq \alpha < 3, 0 \leq \beta < 3, \alpha + \beta > 3 \\ \Theta(nr^3(n)\ln L + nr^{3-\alpha}(n)) & 0 < \alpha < 3, \beta = 3 \\ \Theta(nr^{3-\alpha}(n)) & 0 \leq \alpha < 3, \beta > 3 \\ \Theta(nr^3(n)L^3 + n\log_{r^{-1}(n)}L) & \alpha = 3, \beta = 0 \\ \Theta(nr^3(n)L^{3-\beta} + n\ln^{-1}(r^{-1}(n))) & \alpha = 3, 0 < \beta < 3 \\ \Theta(nr^3(n)\ln L + n\ln^{-1}(r^{-1}(n))) & \alpha = 3, \beta = 3 \\ \Theta(n\ln^{-1}(r^{-1}(n))) & \alpha = 3, \beta > 3 \\ \Theta(n) & \alpha > 3 \end{cases} \quad (27)$$

$$N_c = \begin{cases} \Theta(2nr^\beta(n) - nr^3(n)L^{3-\beta} - nr^{3-\alpha}(n)L^{3-\alpha-\beta}) & 0 \leq \alpha < 3, 0 \leq \beta < 3, \alpha + \beta \neq 3 \\ \Theta(nr^\beta(n) - nr^3(n)L^{3-\beta} + nr^{3-\alpha}(n)\ln(r^{-1}(n)L^{-1})) & 0 \leq \alpha < 3, 0 \leq \beta \leq 3, \alpha + \beta = 3 \\ \Theta(nr^3(n)\ln(r^{-1}(n)L^{-1}) + nr^\beta(n) - nr^{3-\alpha}(n)L^{3-\alpha-\beta}) & 0 < \alpha < 3, \beta = 3 \\ \Theta(nr^3(n) + nr^\beta(n) - nr^{3-\alpha}(n)L^{3-\alpha-\beta}) & 0 \leq \alpha < 3, \beta > 3 \\ \Theta(2n - nr^3(n)L^3 - n\log_{r^{-1}(n)}L) & \alpha = 3, \beta = 0 \\ \Theta(nr^\beta(n) - nr^3(n)L^{3-\beta} + n\ln(r^{-1}(n)L^{-1})(r^\beta(n) - L^{-\beta})) & \alpha = 3, 0 < \beta < 3 \\ \Theta(n\ln(r^{-1}(n)L^{-1})(r^3(n) + r^\beta(n) - L^{-\beta})) & \alpha = 3, \beta = 3 \\ \Theta(nr^3(n) + n\ln(r^{-1}(n)L^{-1})(r^\beta(n) - L^{-\beta})) & \alpha = 3, \beta > 3 \\ \Theta(nr^\beta(n) + nr^{\alpha+\beta-3}(n) - nr^3(n)L^{3-\beta} - nL^{3-\alpha-\beta}) & \alpha > 3, 0 \leq \beta < 3 \\ \Theta(nr^3(n)\ln(r^{-1}(n)L^{-1}) + nr^\alpha(n) - nr^{-\alpha}(n)) & \alpha > 3, \beta = 3 \\ \Theta(nr^3(n) + nr^{\alpha+\beta-3}(n) - nL^{3-\alpha-\beta}) & \alpha > 3, \beta > 3 \end{cases} \quad (28)$$

$$E'[X] = \begin{cases} \Theta(r^3(n)L^{4-\beta} + r^{3-\alpha}(n)L^{4-\alpha-\beta}) & 0 \leq \alpha < 3, 0 \leq \beta < 4, 0 \leq \alpha + \beta < 4 \\ \Theta(r^3(n)L^{4-\beta} + r^{3-\alpha}(n)\ln L) & 0 \leq \alpha < 3, 0 \leq \beta \leq 4, \alpha + \beta = 4 \\ \Theta(r^3(n)L^{4-\beta} + r^{3-\alpha}(n)) & 0 \leq \alpha < 3, 0 \leq \beta < 4, \alpha + \beta > 4 \\ \Theta(r^3(n)\ln L + r^{3-\alpha}(n)) & 0 \leq \alpha < 3, \beta = 4 \\ \Theta(r^{3-\alpha}(n)) & 0 \leq \alpha < 3, \beta > 4 \\ \Theta(r^3(n)L^{4-\beta} + \ln^{-1}(r^{-1}(n))L^{1-\beta}) & \alpha = 3, 0 \leq \beta < 1 \\ \Theta(r^3(n)L^3 + \log_{r^{-1}(n)}L) & \alpha = 3, \beta = 1 \\ \Theta(r^3(n)L^{4-\beta} + \ln^{-1}(r^{-1}(n))) & \alpha = 3, 1 < \beta < 4 \\ \Theta(r^3(n)\ln L + \log_{r^{-1}(n)}L) & \alpha = 3, \beta = 4 \\ \Theta(\ln^{-1}(r^{-1}(n))) & \alpha = 3, \beta > 4 \\ \Theta(r^3(n)L^{4-\beta} + L^{4-\alpha-\beta}) & \alpha > 3, 0 \leq \beta < 4, 0 \leq \alpha + \beta < 4 \\ \Theta(r^3(n)L^{4-\beta} + \ln L) & \alpha > 3, 0 \leq \beta < 4, \alpha + \beta = 4 \\ \Theta(r^3(n)L^{4-\beta}) & \alpha > 3, 0 \leq \beta < 4, \alpha + \beta > 4 \\ \Theta(r^3(n)\ln L) & \alpha > 3, \beta = 4 \\ \Theta(r^3(n)) & \alpha > 3, \beta > 4 \end{cases} \quad (33)$$

n tends to infinity.

$$E'_2[X] = \begin{cases} \Theta(r^{3-\alpha}(n)L^{4-\alpha-\beta}) & 0 \leq \alpha < 3, 0 \leq \alpha + \beta < 4 \\ \Theta(r^{3-\alpha}(n)\ln L) & 0 \leq \alpha < 3, \alpha + \beta = 4 \\ \Theta(r^{3-\alpha}(n)) & 0 \leq \alpha < 3, \alpha + \beta > 4 \\ \Theta(\ln^{-1}(r^{-1}(n))L^{1-\beta}) & \alpha = 3, 0 \leq \alpha + \beta < 4 \\ \Theta(\log_{r^{-1}(n)}L) & \alpha = 3, \alpha + \beta = 4 \\ \Theta(\ln^{-1}(r^{-1}(n))) & \alpha = 3, \alpha + \beta > 4 \\ \Theta(L^{4-\alpha-\beta}) & \alpha > 3, 0 \leq \alpha + \beta < 4 \\ \Theta(\ln L) & \alpha > 3, \alpha + \beta = 4 \\ \Theta(1) & \alpha > 3, \alpha + \beta > 4 \end{cases} \quad (32)$$

When $0 \leq \gamma \leq 1$, $E'_2[X]$ is $n^{\gamma-1}$ times greater than that in (32). (31) and (32) show that if the source nodes are leader nodes, the average number of hops of ad hoc flows is only related to β . If the source nodes are normal nodes, α and β will jointly influence the average number of hops of the ad hoc flows and cellular flows of the source nodes. This is due to the fact that the leader nodes connect more members, which counteracts the influence of the concentration factor α when

Specifically, the distance between source node and destination node will decrease when α or β increases. For leader nodes, when $0 \leq \beta \leq 4$, the average number of hops of ad hoc flows increases when L increases, and decreases when β increases. When β is large, the destination node tends to be closer to the source node. Therefore, when $\beta > 4$, the trend of $E'_1[X]$ has nothing to do with L . For normal nodes, $E'_2[X]$ are influenced by α and β simultaneously. When $0 \leq \alpha < 3$ and $0 \leq \alpha + \beta < 4$, the average number of hops of the ad hoc flows increases when L increases, and decreases when α or β increases. When $\alpha > 3$ or $\alpha + \beta > 4$, L has no relationship with the number of average number of hops.

Since $\gamma > 2$ in the actual network [36][37], we can derive the result of $E'[X]$ as (33).

Finally, we have the following result.

$$\begin{aligned} E[F] &= N_a E[X] V = (n \Pr^\alpha) \times \left(\frac{1}{\Pr^\alpha} E'[X] \right) \times r^3(n) \\ &= \log(n) E'[X]. \end{aligned} \quad (34)$$

E. Network throughput

According to (15), the per-node throughput of ad hoc mode λ_a^n is

$$\lambda_a^n \equiv \Theta \left(\frac{W_a}{E[F]} \right) = \Theta \left(\frac{W_a}{\log(n) E'[X]} \right). \quad (35)$$

Note that if $E[F] = O(1)$, λ_a^n equals to $\Theta(W_a)$, because the average throughput of the ad hoc flows is smaller than W_a .

The relationship between $E'[X]$ and L under different ranges of α and β is analyzed as follows. Note that since $\gamma > 2$ in the actual network [36][37], only the results of $\gamma > 1$ is considered in terms of the number of the ad hoc flows N_a .

In order to better understand the piecewise of throughput as follows, recall that the probability that a node is selected as a member of contact group is proportional to $d_i^{-\alpha}$, the probability that a contact group member will be communicated in a certain time slot is proportional to $d_i^{-\beta}$, and the number of members in the contact group is proportional to $q^{-\gamma}$. Therefore, the probability that a node will be communicated in a certain time slot is proportional to $d_i^{-(\alpha+\beta)}$, i.e., $(\alpha + \beta)$ reveals the communication activity level of the network.

1) $0 \leq \alpha < 3$, $0 \leq \beta < 3$ and $0 \leq \alpha + \beta < 3$: When $L = \Omega(r^{-1}(n))$, $E'[X]$ is dominated by $E'_1[X]$. When $L = O(r^{-1}(n))$, $E'[X]$ is dominated by $E'_2[X]$. Considering that in the unit cube of the communication model in Section II-A1, there is always $L = O(r^{-1}(n))$. Therefore, $E'[X]$ is always dominated by $E'_2[X]$ in this case. So the per-node throughput of ad hoc mode is as follows.

$$\lambda_a^n \equiv \begin{cases} \Theta \left(\frac{W_a}{\log(n)r^{3-\alpha}(n)L^{4-\alpha-\beta}} \right) & L = \Omega \left((\log^{-1}(n)r^{\alpha-3}(n))^{\frac{1}{4-\alpha-\beta}} \right) \\ \Theta(W_a) & L = O \left((\log^{-1}(n)r^{\alpha-3}(n))^{\frac{1}{4-\alpha-\beta}} \right) \end{cases} \quad (36)$$

• When $L = \Omega \left((\log^{-1}(n)r^{\alpha-3}(n))^{\frac{1}{4-\alpha-\beta}} \right)$, the network throughput of ad hoc mode is

$$\begin{aligned} \lambda_a &\equiv N_a \lambda_a^n = \Theta \left(nr^3(n)L^{3-\beta} + nr^{3-\alpha}(n)L^{3-\alpha-\beta} \right) \\ &\cdot \Theta \left(\frac{W_a}{\log(n)r^{3-\alpha}(n)L^{4-\alpha-\beta}} \right) \\ &= \Theta \left(\frac{n^{1-\frac{\alpha}{3}}L^{\alpha-1}W_a}{\log^{1-\frac{\alpha}{3}}(n)} + \frac{nW_a}{\log(n)L} \right). \end{aligned} \quad (37)$$

• When $L = O \left((\log^{-1}(n)r^{\alpha-3}(n))^{\frac{1}{4-\alpha-\beta}} \right)$, the network throughput of ad hoc mode is

$$\begin{aligned} \lambda_a &\equiv N_a \lambda_a^n \\ &= \Theta \left(\log(n)L^{3-\beta}W_a + n^{\frac{\alpha}{3}} \log^{1-\frac{\alpha}{3}}(n)L^{3-\alpha-\beta}W_a \right). \end{aligned} \quad (38)$$

According to (37) and (38), when $L = \Theta \left((\log^{-1}(n)r^{\alpha-3}(n))^{\frac{1}{4-\alpha-\beta}} \right)$, the network throughput of

ad hoc mode is dominant, which is

$$\lambda_a = \Theta \left(\log(n)L^{3-\beta}W_a + n^{\frac{\alpha}{3}} \log^{1-\frac{\alpha}{3}}(n)L^{3-\alpha-\beta}W_a \right). \quad (39)$$

2) $0 \leq \alpha < 3$, $0 \leq \beta < 3$ and $3 < \alpha + \beta < 4$: In this case, $E'[X]$ is dominated by $E'_2[X]$, where $L = O(r^{-1}(n))$. Therefore, the per-node throughput of ad hoc mode is (36).

• When $L = \Omega \left((\log^{-1}(n)r^{\alpha-3}(n))^{\frac{1}{4-\alpha-\beta}} \right)$, the network throughput of ad hoc mode is

$$\begin{aligned} \lambda_a &\equiv N_a \lambda_a^n = \Theta \left(nr^3(n)L^{3-\beta} + nr^{3-\alpha}(n) \right) \\ &\cdot \Theta \left(\frac{W_a}{\log(n)r^{3-\alpha}(n)L^{4-\alpha-\beta}} \right) \\ &= \Theta \left(\frac{n^{1-\frac{\alpha}{3}}L^{\alpha-1}W_a}{\log^{1-\frac{\alpha}{3}}(n)} + \frac{nW_a}{\log(n)L^{4-\alpha-\beta}} \right). \end{aligned} \quad (40)$$

• When $L = O \left((\log^{-1}(n)r^{\alpha-3}(n))^{\frac{1}{4-\alpha-\beta}} \right)$, the network throughput of ad hoc mode is

$$\lambda_a \equiv N_a \lambda_a^n = \Theta \left(\log(n)L^{3-\beta}W_a + n^{\frac{\alpha}{3}} \log^{1-\frac{\alpha}{3}}(n)W_a \right). \quad (41)$$

When $L = \Theta \left((\log^{-1}(n)r^{\alpha-3}(n))^{\frac{1}{4-\alpha-\beta}} \right)$, the network throughput of ad hoc mode is dominant, which is

$$\lambda_a = \Theta \left(\log(n)L^{3-\beta}W_a + n^{\frac{\alpha}{3}} \log^{1-\frac{\alpha}{3}}(n)W_a \right). \quad (42)$$

3) $0 \leq \alpha < 3$, $0 \leq \beta < 3$ and $\alpha + \beta > 4$: In this case, $E'[X]$ is dominated by $E'_1[X]$ when $L = \Omega(r^{\alpha/\beta-4}(n))$, and $E'[X]$ is dominated by $E'_2[X]$ when $L = O(r^{\alpha/\beta-4}(n))$.

• When normal nodes are dominant, $E[F] = \log(n)E[X] = O(1)$. Hence, $\lambda_a^n \equiv \Theta(W_a)$. Note that when $\alpha \equiv \Omega \left(3 + \log_{r(n)} \log(n) \right)$, we have $r^{\alpha/(\beta-4)}(n) \equiv \Omega \left((\log^{-1}(n)r^{-3}(n))^{\frac{1}{4-\beta}} \right)$. However, when $n \rightarrow \infty$, we have $\alpha \equiv O \left(3 + \log_{r(n)} \log(n) \right)$. In this case, $r^{\alpha/(\beta-4)}(n) \equiv O \left((\log^{-1}(n)r^{-3}(n))^{\frac{1}{4-\beta}} \right)$. Thus, the per-node throughput of ad hoc mode is

$$\lambda_a^n \equiv \begin{cases} \Theta \left(\frac{W_a}{\log(n)r^{3-\alpha}(n)L^{4-\beta}} \right) & L = \Omega \left((\log^{-1}(n)r^{-3}(n))^{\frac{1}{4-\beta}} \right) \\ \Theta(W_a) & L = O \left((\log^{-1}(n)r^{-3}(n))^{\frac{1}{4-\beta}} \right) \end{cases} \quad (43)$$

• When $L = \Omega \left((\log^{-1}(n)r^{-3}(n))^{\frac{1}{4-\beta}} \right)$, the network throughput of ad hoc mode is

$$\begin{aligned} \lambda_a &\equiv N_a \lambda_a^n = \Theta \left(nr^3(n)L^{3-\beta} + nr^{3-\alpha}(n) \right) \\ &\cdot \Theta \left(\frac{W_a}{\log(n)r^3(n)L^{4-\beta}} \right) \\ &= \Theta \left(\frac{nW_a}{\log(n)L} + \frac{n^{1+\frac{\alpha}{3}}W_a}{\log \sqrt{3}^{1+\frac{\alpha}{3}}(n)L^{4-\beta}} \right). \end{aligned} \quad (44)$$

• When $L = O \left((\log^{-1}(n)r^{\alpha-3}(n))^{\frac{1}{4-\alpha-\beta}} \right)$, the network throughput of ad hoc mode is

$$\lambda_a \equiv N_a \lambda_a^n = \Theta \left(\log(n)L^{3-\beta}W_a + n^{\frac{\alpha}{3}} \log^{1-\frac{\alpha}{3}}(n)W_a \right). \quad (45)$$

According to (44) and (45), when $L = \Theta \left((\log^{-1}(n)r^{\alpha-3}(n))^{\frac{1}{4-\alpha-\beta}} \right)$, the network throughput of

$$\lambda_a^n \equiv \begin{cases} \Theta\left(\frac{W_a}{\log(n)r^3(n)L^{4-\beta}}\right) \\ \Theta\left(\frac{W_a}{\log(n)L^{4-\alpha-\beta}}\right) \\ \Theta(W_a) \end{cases} \quad L = \Omega\left(\left(\log^{-1}(n)r^{-3}(n)\right)^{\frac{1}{4-\beta}}\right) \text{ and } L = \Omega\left(\log^{-\frac{1}{4-\alpha-\beta}}(n)\right) \quad (50)$$

$$L = \Omega\left(\left(\log^{-1}(n)r^{-3}(n)\right)^{\frac{1}{4-\beta}}\right)$$

$$L = \Omega\left(\log^{-\frac{1}{4-\alpha-\beta}}(n)\right)$$

ad hoc mode is dominant, which is

$$\lambda_a = \Theta\left(\log(n)L^{3-\beta}W_a + n^{\frac{\alpha}{3}}\log^{1-\frac{\alpha}{3}}(n)W_a\right). \quad (46)$$

4) $0 \leq \alpha < 3$, $\beta > 3$ and $3 < \alpha + \beta < 4$: In this case, $E'[X]$ is equal to that of subsection 1) and 2), in which $L = O(r^{-1}(n))$, and $E'[X]$ is dominated by $E'_2[X]$.

• When $L = \Omega\left(\left(\log^{-1}(n)r^{\alpha-3}(n)\right)^{1/4-\alpha-\beta}\right)$, the network throughput of ad hoc mode is

$$\begin{aligned} \lambda_a &\equiv N_a \lambda_a^n = \Theta\left(nr^{3-\alpha}(n)\right) \cdot \Theta\left(\frac{W_a}{\log(n)r^{3-\alpha}(n)L^{4-\alpha-\beta}}\right) \\ &= \Theta\left(\frac{nW_a}{\log(n)L^{4-\alpha-\beta}}\right). \end{aligned} \quad (47)$$

• When $L = \Omega\left(\left(\log^{-1}(n)r^{\alpha-3}(n)\right)^{1/4-\alpha-\beta}\right)$, the network throughput is

$$\lambda_a \equiv N_a \lambda_a^n = \Theta\left(n^{\frac{\alpha}{3}}\log^{1-\frac{\alpha}{3}}(n)W_a\right). \quad (48)$$

Therefore, when $L = \Theta\left(\left(\log^{-1}(n)r^{\alpha-3}(n)\right)^{1/4-\alpha-\beta}\right)$, the network throughput of ad hoc mode is dominant, which is

$$\lambda_a = \Theta\left(n^{\frac{\alpha}{3}}\log^{1-\frac{\alpha}{3}}(n)W_a\right), \quad (49)$$

which reveals that when β is large enough, the destination nodes will gather around the source nodes, which make the network throughput independent of L , and the number of ad hoc transmission depends on the value of α in a certain range.

5) $\alpha > 3$, $0 \leq \beta < 4$ and $3 < \alpha + \beta < 4$: In this case, $E'[X]$ is dominated by $E'_1[X]$ when $L = \Omega\left(r^{-3/\alpha}(n)\right)$, and $E'[X]$ is dominated by $E'_2[X]$ when $L = O\left(r^{-3/\alpha}(n)\right)$. When $L = O\left(r^{-3/\alpha}(n)\right)$, there is always $r^{-3/\alpha}(n) = \Omega\left(\left(\log^{-1}(n)r^{-3}(n)\right)^{1/4-\beta}\right)$. Therefore, the per-node throughput of ad hoc mode is as (50).

• When $L = \Omega\left(\left(\log^{-1}(n)r^{-3}(n)\right)^{1/(4-\beta)}\right)$, the network throughput of ad hoc mode is

$$\begin{aligned} \lambda_a &\equiv N_a \lambda_a^n = \Theta(n) \cdot \Theta\left(\frac{W_a}{\log(n)r^3(n)L^{4-\beta}}\right) \\ &= \Theta\left(\frac{n^2W_a}{\log^2(n)L^{4-\beta}}\right). \end{aligned} \quad (51)$$

• When $L = O\left(\left(\log^{-1}(n)r^{-3}(n)\right)^{1/(4-\beta)}\right)$, and $L = \Omega\left(\log^{-1/(4-\alpha-\beta)}(n)\right)$,

$$\lambda_a \equiv N_a \lambda_a^n = \Theta\left(\frac{nW_a}{\log(n)L^{4-\alpha-\beta}}\right). \quad (52)$$

• When $L = O\left(\log^{-1/(4-\alpha-\beta)}(n)\right)$, the network throughput of ad hoc mode is

$$\lambda_a \equiv N_a \lambda_a^n = \Theta(nW_a). \quad (53)$$

Therefore, when $L = \Theta\left(\log^{-1/4-\alpha-\beta}(n)\right)$, the network throughput of ad hoc mode is dominant, which is

$$\lambda_a = \Theta(nW_a). \quad (54)$$

The result also shows that in this range of parameters, when L breaks the boundary of $\Theta\left(\log^{-1/4-\alpha-\beta}(n)\right)$, the network throughput will have nothing to do with L , and all the nodes will be in ad hoc mode.

6) $\alpha > 3$, $0 \leq \beta < 4$ and $\alpha + \beta > 4$: In this case, $E'[X]$ is dominated by $E'_1[X]$. The per-node throughput of ad hoc mode is

$$\lambda_a^n \equiv \begin{cases} \Theta\left(\frac{W_a}{\log(n)r^3(n)L^{4-\beta}}\right) & L = \Omega\left(\left(\log^{-1}(n)r^{-3}(n)\right)^{\frac{1}{4-\beta}}\right) \\ \Theta(W_a) & L = O\left(\left(\log^{-1}(n)r^{-3}(n)\right)^{\frac{1}{4-\beta}}\right) \end{cases} \quad (55)$$

• When $L = \Omega\left(\left(\log^{-1}(n)r^{-3}(n)\right)^{1/4-\beta}\right)$, the network throughput of ad hoc mode is

$$\begin{aligned} \lambda_a &\equiv N_a \lambda_a^n = \Theta(n) \cdot \Theta\left(\frac{W_a}{\log(n)r^3(n)L^{4-\beta}}\right) \\ &= \Theta\left(\frac{n^2W_a}{\log^2(n)L^{4-\beta}}\right). \end{aligned} \quad (56)$$

• When $L = O\left(\left(\log^{-1}(n)r^{-3}(n)\right)^{1/4-\beta}\right)$, the network throughput of ad hoc mode is

$$\lambda_a \equiv N_a \lambda_a^n = \Theta(nW_a). \quad (57)$$

Therefore, when $L = \Theta\left(\left(\log^{-1}(n)r^{-3}(n)\right)^{1/4-\beta}\right)$, the network throughput of ad hoc mode is dominant, which is

$$\lambda_a = \Theta(nW_a). \quad (58)$$

The result shows that the increase of α influences the distribution of the destination nodes. When L breaks the boundary of $\Theta\left(\left(\log^{-1}(n)r^{-3}(n)\right)^{1/4-\beta}\right)$, the network throughput will no longer be related to L , and all the nodes will be in ad hoc mode.

7) $\alpha > 3$ and $\beta > 4$: In this case, $E'[X] = \Theta(r^3(n))$, and $E[F] = \log(n)E'[X] = O(1)$ when $n \rightarrow \infty$. Therefore, the per-node throughput of ad hoc mode is

$$\lambda_a^n \equiv \Theta(W_a). \quad (59)$$

When α and β are large, the destination nodes are close to the source nodes. As a result, the number of hops are always smaller than L , and all of the nodes transmit in ad hoc mode. In this case, the network throughput has nothing to do with L . The network throughput of ad hoc mode is

$$\lambda_a \equiv N_a \lambda_a^n = \Theta(n) \cdot \Theta(W_a) = \Theta(nW_a). \quad (60)$$

In conclusion, the aggregation of destination nodes (i.e. the value of $\alpha + \beta$) is the main factor affecting the network throughput. When the distribution of destination nodes is

sparse, the network throughput has complex relationships with hop threshold L , the number of nodes n , and the bandwidth W_a , as shown in (39)(42)(46). When the destination nodes gather around the source nodes, the flows in the network are generally ad hoc flows. The hop threshold L has limited impact on the network throughput, and the throughput is only positively related to the number of nodes n and bandwidth W_a , as shown in (49)(54)(57)(60). Furthermore, as shown in (54)(57)(60), when the destination nodes have strong aggregation to the source nodes, the network throughput will be in direct proportion to the product of n and W_a .

IV. NUMERICAL RESULTS AND ANALYSIS

In this section, the theoretical results in Section III are verified by numerical results, and the relationship between parameters and network throughput is analyzed through the numerical results. Besides, the network throughput of 100 to 10000 UAVs is simulated by MATLAB to verify the rationality of the theoretical results.

According to the theoretical results derived above, Fig. 4 shows the relation between the threshold L and the throughput with different values of α and β . We consider four typical conditions, where $n = 100$, $W_a = 1$, and the optimal L are identified.

In Fig. 4(a), where $0 \leq \alpha < 3$ and $0 \leq \alpha + \beta < 4$, the optimal L is relatively small. Since the values of α and β are small, there are more long-distance flows. Besides, because the leader nodes have large contact groups, these long-distance flows are more likely to be sent by leader nodes and their hops are more likely to be larger than L , which means that most of the long-distance flows are cellular flows. In this case, the throughput of the ad hoc network is dominated by flows of normal nodes.

In Fig. 4(b), where $0 \leq \alpha < 3$, $0 \leq \beta < 3$ and $\alpha + \beta > 4$, the optimal L is relatively large. At this time, because α and β are small, there are still many long-distance flows from the leader nodes. However, since L increases, the number of long-distance flows with ad hoc mode increases, and the throughput tends to be dominated by leader nodes.

In Fig. 4(c), where $\alpha > 3$, $0 \leq \beta < 4$ and $3 < \alpha + \beta < 4$, there are two optimal L , which shows that the value of L determines the type of nodes that dominate the throughput. When $L = \Omega \left((\log^{-1}(n)r^{-3}(n))^{1/(4-\beta)} \right)$, the throughput is dominated by leader nodes. When $L = O \left((\log^{-1}(n)r^{-3}(n))^{1/(4-\beta)} \right)$ and $L = \Omega \left(\log^{-1/(4-\alpha-\beta)}(n) \right)$, the throughput is dominated by normal nodes. Because α is large, the aggregation of contact groups of source nodes is high. However, β and $\alpha + \beta$ are still small. Thus, it is still possible for source nodes to communicate with contact group nodes with a long distance. Due to the large number of contact group members of leader nodes, it is more likely that such long-distance flows will be sent by leader nodes. It can be explained that when L is large, more long-distance flows sent by leader nodes are transmitted by ad hoc mode, which dominates the network throughput. When L is small, leader nodes prefer cellular mode, so that the throughput of ad hoc flows is dominated by normal nodes.

In Fig. 4(d), as α increases, the aggregation of the contact groups is further improved. It is more likely that the number of hops of long-distance flows is less than L , so that the throughput of ad hoc flows is dominated by leader nodes again.

The theoretical results above show that there is an optimal value of L to maximize the average throughput of UAV network, which is of great significance to the design of hybrid UAV network. For example, when the number of UAVs and the capabilities of UAVs are determined, the parameters α , β and γ can be determined by analyzing the routing table and the topological relation of UAV network. With such parameters, we can determine the value of routing strategy L in hybrid UAV network to maximize the throughput of UAV network.

In order to verify the theoretical results through simulation, firstly, the Bat Algorithm (BA) algorithm is applied to generate a scale-free network which has the same setting as the models in Section II. Taking 100 nodes as an example, the contact groups and communication relationships of each node are shown in Fig. 5 and Fig. 6.

Fig. 5 is the contact group selection when $n = 100$, $\alpha = 1$, $\beta = 0.5$, and $\gamma = 2$. The UAVs are randomly distributed in the 3D space. The selection of the contact group members of the source nodes follows the power-law distribution with parameter α . In the simulation of Fig. 5, the threshold q_0 is set to be 17.33. The source node of Fig. 5(a) is a leader node with 25 social group members. The source node of Fig. 5(b) is a normal node with 5 social group members.

Fig. 6 illustrates the contact group selection related to parameter α , the communication selection in the contact group related to parameter β , and the final communication relationship. The three sub-figures in Fig. 6 are all directed graphs. The evolution process is revealed from the first sub-figure to the last sub-figure.

Then, according to the L -routing scheme, whether a transmission adopts ad hoc mode or cellular mode is determined. Taking the number of nodes n as the variable, the results of average hops and throughput under different parameters of α , β and γ are simulated, which is shown in Fig. 7(a) and Fig. 7(b).

Fig. 7(a) illustrates the average number of hops of ad hoc flows under different parameters α and β . Fig. 7(b) shows the throughput of the ad hoc flows. L is selected in the optimal range to maximize the throughput of ad hoc flows, and the bandwidth of ad hoc mode is set to be $W_a = 1$. There are the following observations.

1) When the values of α and β , or the sum of them increase, the average number of hops of flows decreases correspondingly, and the throughput of UAV network increases. This is due to the fact that α and β affect the location distribution of the destination nodes from the source node. When α or β is large, or the sum of them exceeds a certain range, the destination nodes will be highly clustered around the source node, so that the average number of hops of ad hoc flows are reduced, and the network throughput increases accordingly.

2) Within a certain range of α and β , the size of L will affect the type of the dominant nodes. For example, when $0 \leq \alpha < 3$, $0 \leq \beta < 3$ and $\alpha + \beta > 4$, the simulation results of the average number of hops and throughput are in good

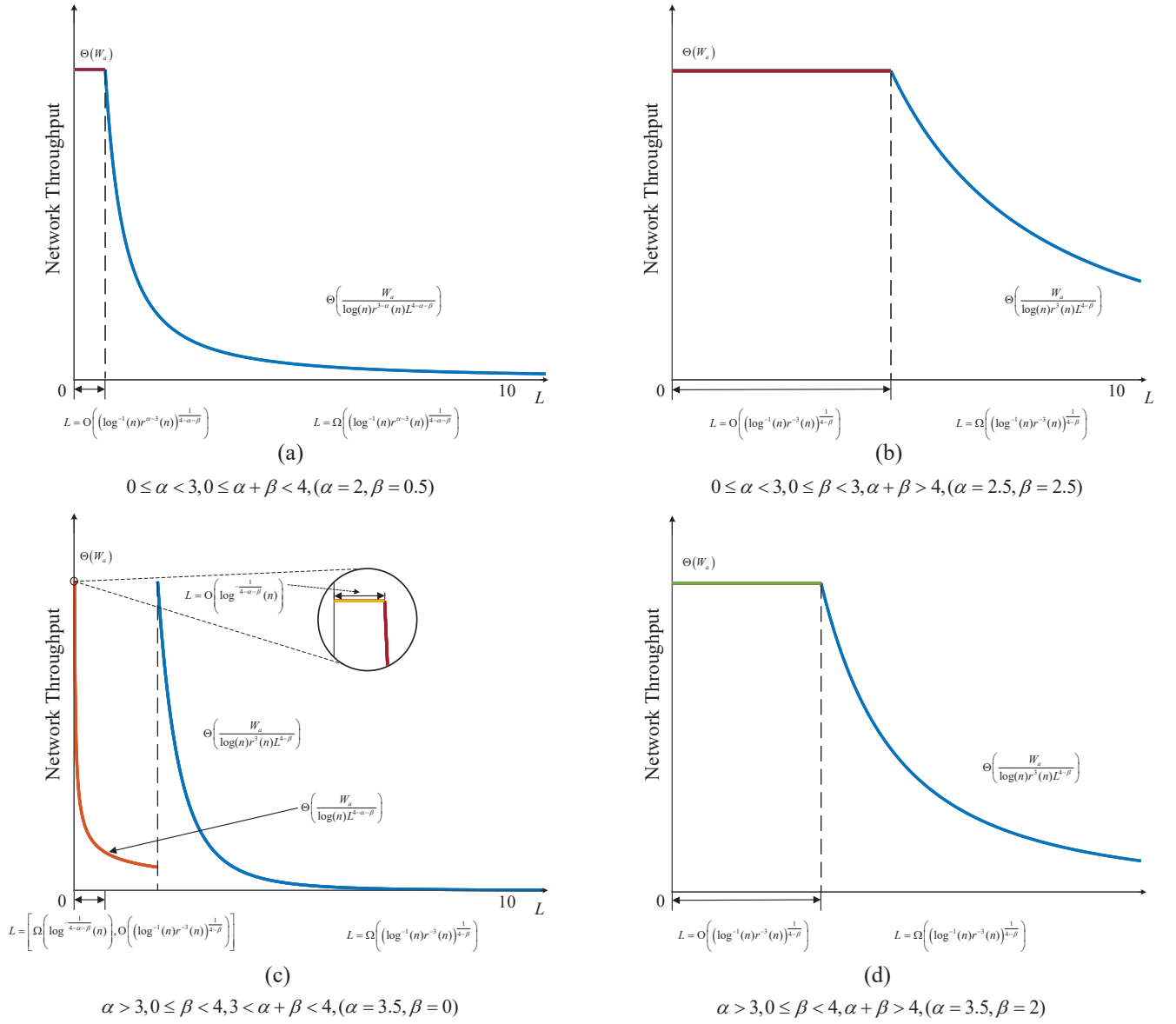


Fig. 4. The relationship between L and throughput of ad hoc network

agreement with the theoretical results, which shows that the flows of normal nodes is dominant in the network.

3) The introduction of the cellular transmission mode improves the throughput of the scale-free UAV network, compared with the throughput of pure ad hoc network studied in [24]. Fig. 7(a) shows that as n increases, the average number of hops of ad hoc flows in hybrid UAV network is smaller than that of pure ad hoc network. Correspondingly, Fig. 7(b) shows that as n increases, the throughput of hybrid UAV network is higher than that of pure ad hoc network. This is due to the fact that for the flows with the number of hops larger than L , the nodes will directly connect to BSs and exploit the resources of cellular network for transmission. Therefore, the number of ad hoc flows is reduced, and the resources of ad hoc network are saved, so that the network throughput is improved.

V. CONCLUSION

In this paper, aiming at improving the throughput of UAV network, the hybrid UAV network with scale-free topology is studied. Besides, the impact of various parameters on the network throughput is analyzed. The optimal hop threshold L for the selection of ad hoc or cellular transmission mode is derived, which is a function of the number of nodes and scale-free parameters. This paper will provide guidance for the architecture design and protocol design for the future UAV network.

APPENDIX A

According to [24] and law of large numbers (LLN), we have

$$\frac{d_k^{-\alpha} \sigma_{q-1}(\mathbf{d}_n^{\bar{k}})}{\sigma_q(\mathbf{d}_n)} = \frac{q}{n}. \quad (61)$$

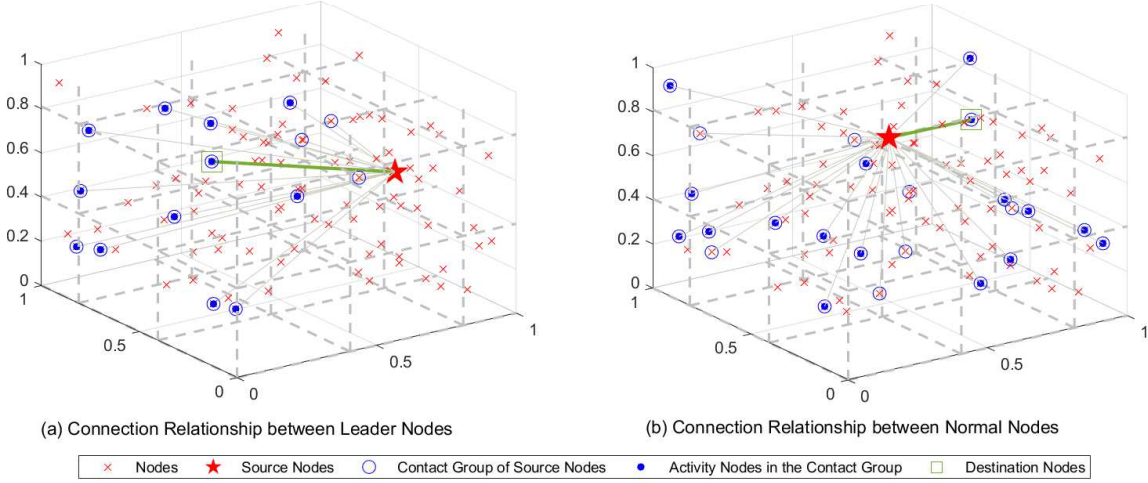


Fig. 5. The contact groups of leader nodes and normal nodes

Therefore, (21) and (22) can be simplified as

$$\Pr_1^a = \sum_{x=1}^L \sum_{l=1}^{4x^2+2} \sum_{o_k \in c_l} \sum_{q=q_0+1}^{n-1} \frac{q^{-\gamma+1} d_k^{-\beta}}{n\sigma_1(\mathbf{q})\sigma_1(\mathbf{d}_q)}. \quad (62)$$

$$\Pr_1^c = \sum_{x=L+1}^{r^{-1}(n)} \sum_{l=1}^{4x^2+2} \sum_{o_k \in c_l} \sum_{q=q_0+1}^{n-1} \frac{q^{-\gamma+1} d_k^{-\beta}}{n\sigma_1(\mathbf{q})\sigma_1(\mathbf{d}_q)}. \quad (63)$$

According to LLN, we have

$$\frac{1}{q} \sigma_1(\mathbf{d}_q) = E[\mathbf{d}_q]. \quad (64)$$

Therefore,

$$\sum_{q=q_0}^{n-1} \frac{q^{-\gamma+1}}{\sigma_1(\mathbf{d}_q)} = \frac{1}{E[\mathbf{d}_q]} \sum_{q=q_0}^{n-1} q^{-\gamma}. \quad (65)$$

According to (9), we have

$$E[\mathbf{d}_q] \equiv E\left[\left\{d_{g_1}^{-\beta}, d_{g_2}^{-\beta}, \dots, d_{g_q}^{-\beta}\right\}\right], \quad (66)$$

where d_{g_i} ($i = 1, 2, \dots, q$) is the the distance between source and destination, which can be replaced by $xr(n)$, so we have

$$\begin{aligned} E[\mathbf{d}_q] &\equiv \sum_{x=1}^{r^{-1}(n)} \Pr(X=x)(xr(n))^{-\beta} \\ &= r(n)^{-\beta}. \end{aligned} \quad (67)$$

Therefore, with (65) and (67), \Pr_1^a can be simplified as

$$\Pr_1^a \equiv \frac{r^\beta(n)}{n} \sum_{x=1}^L \sum_{l=1}^{4x^2+2} \sum_{o_k \in c_l} d_k^{-\beta} \sum_{q=q_0+1}^{n-1} \frac{q^{-\gamma}}{\sigma_1(\mathbf{q})}. \quad (68)$$

If $\gamma > 1$, $\sum_{q=q_0}^{n-1} q^{-\gamma}$ and $\sigma_1(\mathbf{q})$ are all partial sum of the Riemann Zeta function, which has the following relations.

$$\sum_{q=q_0}^{n-1} q^{-\gamma} \leq \sigma_1(\mathbf{q}) \leq \zeta(\gamma) \equiv \Theta(1). \quad (69)$$

Therefore, when $\gamma > 1$, according to (69), $q^{-\gamma}/\sigma_1(\mathbf{q}) = 1$.

\Pr_1^a can be derived as follows

$$\Pr_1^a \equiv \frac{r^\beta(n)}{n} \sum_{x=1}^L \sum_{l=1}^{4x^2+2} \sum_{o_k \in c_l} d_k^{-\beta}. \quad (70)$$

For $0 \leq \gamma \leq 1$, it's obvious that

$$\sum_{q=q_0+1}^{n-1} q^{-\gamma} = \Theta(\sigma_1(\mathbf{q})) = \Theta(n^{1-\gamma}/(1-\gamma)). \quad (71)$$

Thus, \Pr_1^a is still equivalent to (70) when $0 \leq \gamma \leq 1$, i.e., \Pr_1^a has the same form when γ varies.

In (70), $\sum_{l=1}^{4x^2+2} \sum_{o_k \in c_l} (\cdot)$ represents the number of nodes in the small cubes with x hops on average, which has the same order as

$$Nn(r(n))^3 = (4x^2 + 2) n(r(n))^3. \quad (72)$$

Therefore, with (72) and Riemann integral, we have

$$\begin{aligned} \Pr_1^a &\equiv \frac{r^\beta(n)}{n} \sum_{x=1}^L \sum_{l=1}^{4x^2+2} \sum_{o_k \in c_l} d_k^{-\beta} \equiv (r(n))^3 \sum_{x=1}^L \left(x^{2-\beta} + x^{-\beta}\right) \\ &\equiv (r(n))^3 \int_1^L \left(v^{2-\beta} + v^{-\beta}\right) dv. \end{aligned} \quad (73)$$

Thus, the simplified form of \Pr_1^a is as follows.

$$\Pr_1^a \equiv \begin{cases} \Theta\left(r^3(n)L^{3-\beta}\right) & 0 \leq \beta < 3 \\ \Theta\left(r^3(n) \ln L\right) & \beta = 3 \\ \Theta\left(r^3(n)\right) & \beta > 3 \end{cases} \quad (74)$$

The simplified form of \Pr_1^c can be derived similarly, which is

$$\Pr_1^c \equiv \begin{cases} \Theta\left(r^\beta(n) - r^3(n)L^{3-\beta}\right) & 0 \leq \beta < 3 \\ \Theta\left(r^3(n) \ln\left(\frac{1}{Lr(n)}\right)\right) & \beta = 3 \\ \Theta\left(r^3(n)\right) & \beta > 3 \end{cases} \quad (75)$$

APPENDIX B

In (23) and (24), the term $d_k^{-\alpha} \sigma_{q-1}(\mathbf{d}_n^k)$ can be expanded as follows.

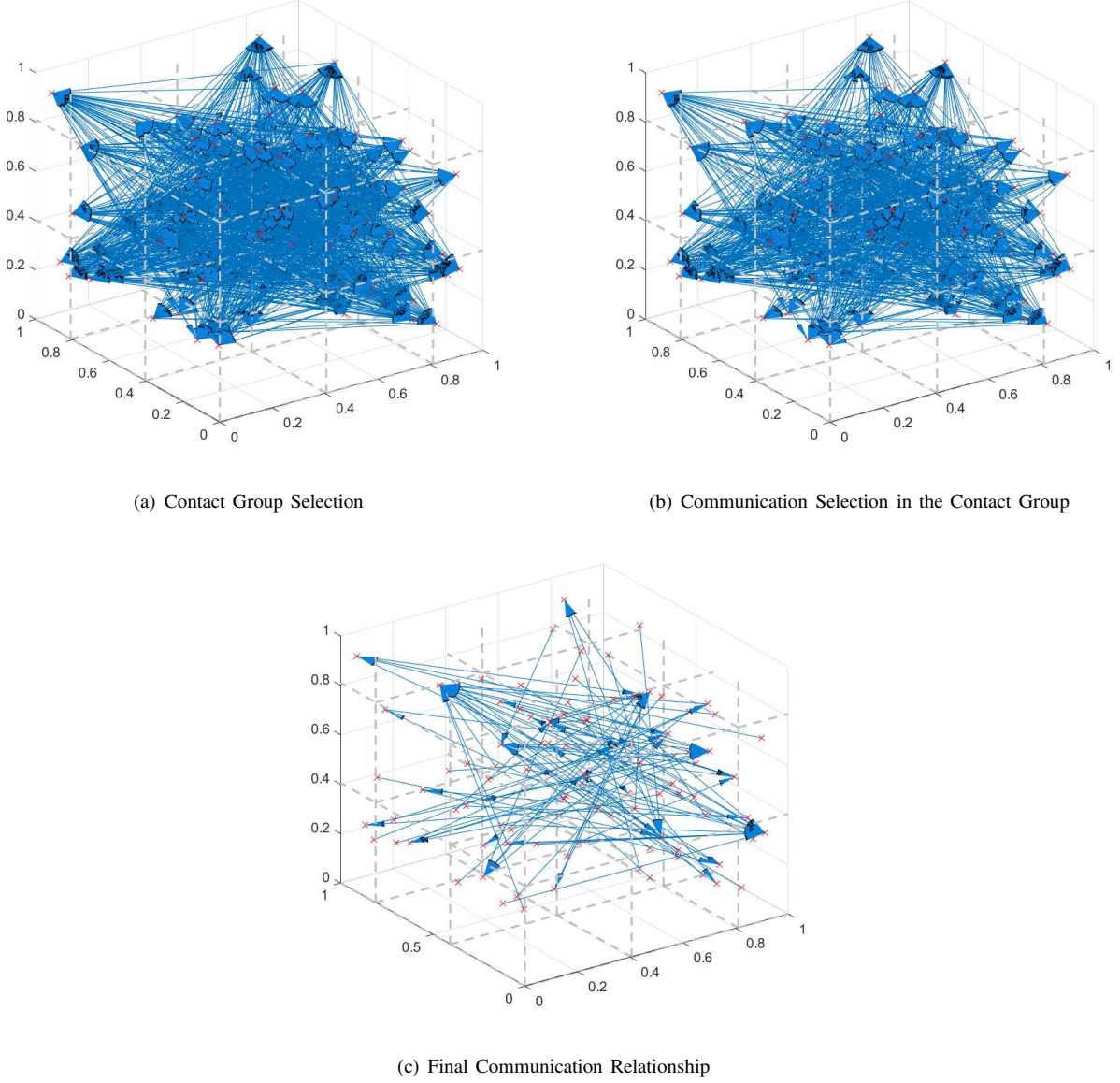


Fig. 6. The contact group selection, the communication selection in the contact group, and the final communication relationship

$$d_k^{-\alpha} \sigma_{q-1}(\mathbf{d}_n^{\bar{k}}) = d_k^{-\alpha} \left(\sigma_{q-1}(\mathbf{d}_n) - d_k^{-\alpha} \sigma_{q-2}(\mathbf{d}_n^{\bar{k}}) \right) \leq d_k^{-\alpha} \sigma_{q-1}(\mathbf{d}_n). \quad (76)$$

Hence, the upper bound of $d_k^{-\alpha} \sigma_{q-1}(\mathbf{d}_n^{\bar{k}})$ is $d_k^{-\alpha} \sigma_{q-1}(\mathbf{d}_n)$. According to Lemma 4 in [35], when $q \leq q_0$, we have

$$\frac{\sigma_{q-1}(\mathbf{d}_n)}{\sigma_q(\mathbf{d}_n)} \equiv \frac{1}{\sigma_1(\mathbf{d}_n)} \Theta\left(\frac{nq}{n-q+1}\right), \quad (77)$$

and

$$\Theta\left(\frac{nq}{n-q+1}\right) = \Theta(q) = \Theta(1). \quad (78)$$

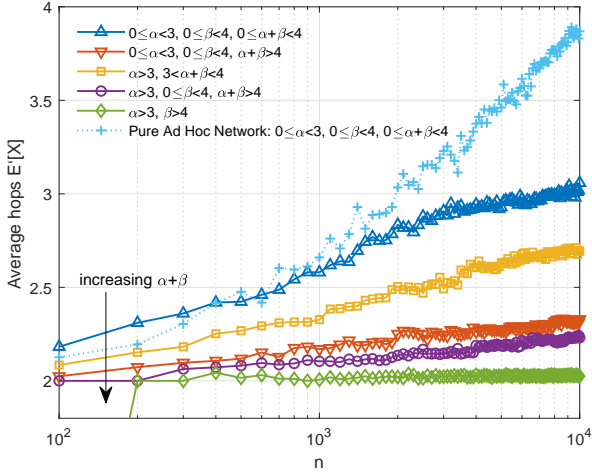
Hence, when $q \leq q_0$, Pr_2^a is equivalent to

$$\begin{aligned} \text{Pr}_2^a &\equiv \sum_{x=1}^L \sum_{l=1}^{4x^2+2} \sum_{o_k \in c_l} \sum_{q=1}^{q_0} \frac{q^{-\gamma} d_k^{-\alpha-\beta} \sigma_{q-1}(\mathbf{d}_n)}{\sigma_1(\mathbf{q}) \sigma_1(\mathbf{d}_q) \sigma_q(\mathbf{d}_n)} \\ &\equiv \sum_{x=1}^L \sum_{l=1}^{4x^2+2} \sum_{o_k \in c_l} \frac{d_k^{-\alpha-\beta}}{\sigma_1(\mathbf{q}) \sigma_1(\mathbf{d}_n)} \sum_{q=1}^{q_0} \frac{q^{-\gamma}}{\sigma_1(\mathbf{d}_q)}. \end{aligned} \quad (79)$$

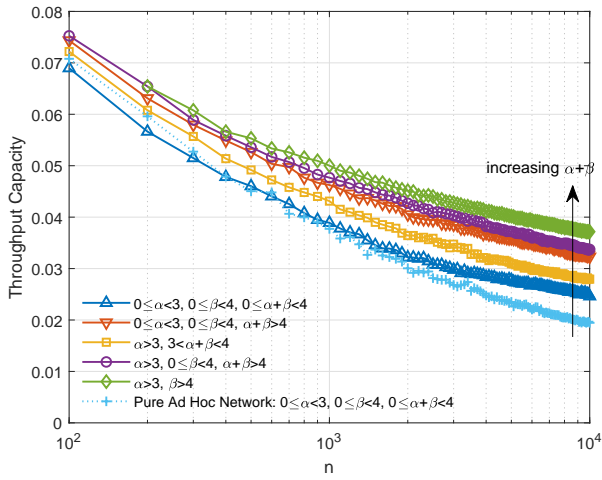
According to (44) in [21], we have

$$\sum_{q=1}^{q_0} q^{-\gamma} / \sigma_1(\mathbf{d}_q) \equiv r^\beta(n), \quad (80)$$

which is substituted into (79). Using integral transformation techniques, we have



(a) The relationship between the number of nodes and the average number of hops of ad hoc network



(b) The relationship between the number of nodes and throughput of ad hoc network

Fig. 7. The relationship between parameters of UAV network

$$\begin{aligned}
 \Pr_2^a &\equiv \frac{r^\beta(n)}{\sigma_1(\mathbf{q})\sigma_1(\mathbf{d}_n)} \sum_{x=1}^L \sum_{l=1}^{4x^2+2} \sum_{o_k \in c_l} d_k^{-\alpha-\beta} \\
 &\equiv \frac{nr^{3-\alpha}(n)}{\sigma_1(\mathbf{q})\sigma_1(\mathbf{d}_n)} \sum_{x=1}^L (x^{2-\alpha-\beta} + x^{-\alpha-\beta}) \\
 &\equiv \frac{nr^{3-\alpha}(n)}{\sigma_1(\mathbf{q})\sigma_1(\mathbf{d}_n)} \int_1^L (v^{2-\alpha-\beta} + v^{-\alpha-\beta}) dv.
 \end{aligned} \tag{81}$$

According to (16) in [24], we have

$$\sigma_1(\mathbf{d}_n) \equiv \begin{cases} \Theta(n) & 0 \leq \alpha < 3 \\ \Theta(n \ln(r^{-1}(n))) & \alpha = 3 \\ \Theta(nr^{3-\alpha}(n)) & \alpha > 3 \end{cases} \tag{82}$$

Besides, there is the following relation.

$$\sigma_1(\mathbf{q}) = \sum_{q=1}^{n-1} q^{-\gamma} \equiv \begin{cases} \Theta(1) & \gamma > 1 \\ \Theta(n^{1-\gamma}) & 0 \leq \gamma \leq 1 \end{cases} \tag{83}$$

Substituting (81) and (82) into (83), the values of \Pr_2^a are

revealed in Table I. Similarly, using the techniques of integral transformation, the values of \Pr_2^c are revealed in Table II.

REFERENCES

- [1] S. Hayat, E. Yanmaz and R. Muzaffar, "Survey on Unmanned Aerial Vehicle Networks for Civil Applications: A Communications Viewpoint," in *IEEE Communications Surveys & Tutorials*, vol. 18, no. 4, pp. 2624–2661, Fourthquarter 2016.
- [2] L. Gupta, R. Jain, and G. Vaszkun, "Survey of Important Issues in UAV Communication Networks," in *IEEE Communications Surveys & Tutorials*, vol. 18, no. 2, pp. 1123–1152, Secondquarter 2016.
- [3] P. Smith, D. Hutchison, J. P.G. Sterbenz, et al. "Network resilience: a systematic approach," in *IEEE Communications Magazine*, vol. 49, no. 7, pp. 88–97, July 2011.
- [4] Z. Yuan, J. Jin, L. Sun, et al. "Ultra-Reliable IoT Communications with UAVs: A Swarm Use Case," in *IEEE Communications Magazine*, vol. 56, no. 12, pp. 90–96, December 2018.
- [5] M. M. Azari, F. Rosas, K. Chen, et al. "Ultra Reliable UAV Communication Using Altitude and Cooperation Diversity," in *IEEE Transactions on Communications*, vol. 66, no. 1, pp. 330–344, Jan. 2018.
- [6] M. Faloutsos, P. Faloutsos, C. Faloutsos. "On power-law relationships of the internet topology," in *ACM SIGCOMM computer communication review*, vol. 29, no. 4, pp. 251–262, 1999.
- [7] S. Boccaletti, V. Latora, Y. Moreno, et al. "Complex networks: Structure and dynamics," in *Physics reports*, vol. 424, no. 4, pp. 175–308, 2006.
- [8] J. Fan, D. Li, R. Li, et al. "Analysis on MAV/UAV cooperative combat based on complex network," in *Defence Technology*, vol. 16, no. 1, pp. 150–157, 2020.
- [9] W. Xiaohong, Y. Zhang, W. Lizhi, et al. "Robustness evaluation method for unmanned aerial vehicle swarms based on complex network theory," in *Chinese Journal of Aeronautics*, vol. 33, no. 1, pp. 352–364, 2020.
- [10] S. Singh, M. M. Kokar, "Simulation of Scale-Free Correlation in Swarms of UAVs," *International Conference on Complex Systems*, Springer, Cham, pp. 91–97, 2018.
- [11] L. K. Gallos, R. Cohen, P. Argyrakis, et al. "Stability and topology of scale-free networks under attack and defense strategies," in *Physical review letters*, vol. 94, no. 18, pp. 188701, 2005.
- [12] R. Cohen, K. Erez, D. Ben-Avraham, et al. "Breakdown of the internet under intentional attack," in *Physical review letters*, vol. 86, no. 16, pp. 3682, 2001.
- [13] H. T. Tran, "A complex networks approach to designing resilient system-of-systems," *Georgia Institute of Technology*, 2015.
- [14] Q. Chen, H. Wang, N. Liu. "Integrating Networking, Storage, and Computing for Resilient Battlefield Networks," *IEEE Communications Magazine*, vol. 57, no. 8, pp. 56–63, 2019.
- [15] B. Liu, F. Qiu, Y. Cao, et al. "Maximizing Resilient Throughput in Peer-to-Peer Network," *Commun. Netw.*, vol. 3, no. 3, pp. 168–183, 2011.
- [16] X. Yuan, Z. Feng, W. Xu, et al. "Capacity Analysis of UAV Communications: Cases of Random Trajectories," in *IEEE Transactions on Vehicular Technology*, vol. 67, no. 8, pp. 7564–7576, Aug. 2018.
- [17] P. Li and J. Xu, "Fundamental Rate Limits of UAV-Enabled Multiple Access Channel With Trajectory Optimization," in *IEEE Transactions on Wireless Communications*, vol. 19, no. 1, pp. 458–474, Jan. 2020.
- [18] V. V. Chetlur and H. S. Dhillon, "Downlink Coverage Analysis for a Finite 3-D Wireless Network of Unmanned Aerial Vehicles," in *IEEE Transactions on Communications*, vol. 65, no. 10, pp. 4543–4558, Oct. 2017.
- [19] N. Gao, X. Li, S. Jin, et al. "3-D Deployment of UAV Swarm for Massive MIMO Communications," in *IEEE Journal on Selected Areas in Communications*, pp. 1–1, Jun. 2021.
- [20] Z. Wei, H. Wu, X. Yuan, et al. "Achievable Capacity Scaling Laws of Three-Dimensional Wireless Social Networks," in *IEEE Transactions on Vehicular Technology*, vol. 67, no. 3, pp. 2671–2685, March 2018.
- [21] M. Karimzadeh Kiskani, B. Azimdoost and H. R. Sadjadpour, "Effect of contact groups on the Capacity of Wireless Networks," in *IEEE Transactions on Wireless Communications*, vol. 15, no. 1, pp. 3–13, Jan. 2016.
- [22] B. Azimdoost, H. R. Sadjadpour and J. J. Garcia-Luna-Aceves, "Capacity of Wireless Networks with Social Behavior," in *IEEE Transactions on Wireless Communications*, vol. 12, no. 1, pp. 60–69, January 2013.
- [23] R. Hou, Y. Cheng, J. Li, et al. "Capacity of Hybrid Wireless Networks With Long-Range Social Contacts Behavior," in *IEEE/ACM Transactions on Networking*, vol. 25, no. 2, pp. 834–848, April 2017.

- [24] Z. Wang, Z. Wei and Z. Feng, "Capacity of Three-Dimensional Scale Free Wireless Networks," *2018 IEEE/CIC International Conference on Communications in China (ICCC)*, pp. 288–292, 2018.
- [25] A. A. Khuwaja, Y. Zhu, G. Zheng, et al. "Performance Analysis of Hybrid UAV Networks for Probabilistic Content Caching," in *IEEE Systems Journal*, pp.1–12, Aug. 2020.
- [26] A. Agarwal, P. R. Kumar, "Capacity bounds for ad hoc and hybrid wireless networks," in *ACM SIGCOMM Computer Communication Review*, vol. 34, no. 3, pp. 71–81, 2004.
- [27] Z. Wei, H. Wu, X. Yuan, et al. "Achievable Capacity Scaling Laws of Three-Dimensional Wireless Social Networks," *IEEE Transactions on Vehicular Technology*, vol. 67, no. 3, pp. 2671–2685, Mar. 2018.
- [28] F. Xue, P. R. Kumar. "Scaling laws for ad hoc wireless networks: an information theoretic approach," in *Foundations and Trends in Networking*, vol. 1, no. 2, pp. 145–270, 2006.
- [29] P. Gupta, P. R. Kumar. "Internets in the sky: The capacity of three-dimensional wireless networks," in *Communications in Information and Systems*, vol. 1, no. 1, pp. 33–50, 2001.
- [30] F. Xue and P. R. Kumar, "Scaling Laws for Ad Hoc Wireless Networks: An Information Theoretic Approach," *Foundations and Trends in Networking*, vol. 1, no. 2, pp.145–270, 2006.
- [31] C. Chau, M. Chen and S. C. Liew, "Capacity of Large-Scale CSMA Wireless Networks," in *IEEE/ACM Transactions on Networking*, vol. 19, no. 3, pp. 893–906, June 2011.
- [32] P. Li, C. Zhang, and Y. Fang, "Capacity and delay of hybrid wireless broadband access networks," in *IEEE Journal on Selected Areas in Communications*, vol. 27, no. 2, pp. 117–125, February 2009.
- [33] M. K. Kiskani, H. Sadjadpour and M. Guizani, "Social interaction increases capacity of wireless networks," *2013 9th International Wireless Communications and Mobile Computing Conference (IWCMC)*, pp. 467–472, 2013.
- [34] P. Li, C. Zhang and Y. Fang, "Capacity and delay of hybrid wireless broadband access networks," in *IEEE Journal on Selected Areas in Communications*, vol. 27, no. 2, pp. 117–125, February 2009.
- [35] B. Azimdoost and H. R. Sadjadpour, "Capacity of scale free wireless networks," *2012 IEEE Global Communications Conference (GLOBECOM)*, pp. 2379–2384, 2012.
- [36] K. Choromanski, M. Matuszak, J. Miekisz. "Scale-free graph with preferential attachment and evolving internal vertex structure," *Journal of Statistical Physics*, vol. 151, no. 6, pp. 1175–1183, 2013.
- [37] J. P. Onnela, J. Saramaki, J. Hyvonen, et al. "Structure and tie strengths in mobile communication networks," *Proceedings of the national academy of sciences*, vol. 104, no. 18, pp. 7332–7336, 2007.











